Long Range Collisional Energy Transfer from Highly Vibrationally Excited Pyrazine to CO Bath Molecules: Excitation of the v = 1 CO Vibrational Level†

N. Seiser,‡ K. Kavita, and G. W. Flynn*

Department of Chemistry and Columbia Center for Integrated Science and Engineering, Columbia University, New York, New York 10027

Received: December 9, 2002; In Final Form: April 11, 2003

Collisional energy transfer from highly vibrationally excited pyrazine to CO bath molecules has been studied by use of an infrared diode laser to probe the vibrational, rotational, and translation degrees of freedom of scattered CO molecules. Here the excitation of the CO ($v = 1$) bath molecule vibrational state is investigated after a collision with highly excited, vibrationally "hot" pyrazine. Only a small amount of rotational and translational excitation accompanies the production of CO ($v = 1$), implicating a "soft" collision, long-range force energy transfer mechanism. The amount of CO scattered into the $v = 1$ state at 2170 cm^{-1} is small when compared to the amount of CO_2 scattered into the analogous 00^01 level of CO_2 at 2349 cm^{-1} by collisions with pyrazine molecules having 40 640 cm^{-1} of internal vibrational energy.

Introduction

Collisional energy transfer from highly excited molecules has mainly been studied to unravel the role of this process in unimolecular reactions, which are important in such fields as combustion and atmospheric chemistry. Most experimental and theoretical studies focus on monitoring the collisional deactivation of the highly excited donor and yield quantities such as the average energy transferred. More recently, efforts have been focused on obtaining the energy transfer distribution function $P(E, E')$, which is the probability for a donor to lose an amount of energy $\Delta E = E - E'$ in a collision. Among the experimental methods employed to determine these energy transfer distribution functions are kinetically controlled selective ionization (KCSI),[1−3] infrared fluorescence (IRF),[4] and infrared diode laser probing.[5−9] In parallel with these experimental techniques, classical trajectory calculations by Luther and Lenzer and coworkers,[2,3,10] by Bernshtein and Oref,[11,12] and by Higgins et al.[13] have provided a detailed picture of the collisional energy transfer process in addition to the average energy transferred. Clary et al.[14] have also investigated energy transfer in highly excited benzene/rare gas collisions using vibrational close coupling, infinite-order sudden quantum scattering, and classical trajectory methods. Recently, experimental methods that prepare selected quantum states of the highly vibrationally excited donor, such as the pump−dump−probe technique,[15] have been used to obtain a more detailed, quantum-state-resolved picture of some collisional relaxation processes.

The diode laser probe technique, which has been developed[5] and successfully used[6−9] to study the collisional transfer of energy from highly vibrationally excited molecules to small bath molecules, provides unambiguous quantum-state-resolved information about the collisional excitation of the bath molecule. Through the use of this experimental approach, two dominant energy-transfer mechanisms have been found to control the collisional deactivation of highly vibrationally excited pyrazine,[6,9] hexafluorobenzene,[8] and methylpyrazine.[16] Most of these studies have focused on scattering events that result in the excitation of the rotational and translational degrees of freedom of bath molecules such as CO_2[7,8] and CO[17] in their ground vibrational state, which represent the dominant short-range repulsive-force energy-transfer mechanism. However, earlier studies of the vibrational excitation of CO_2 after collisions with highly vibrationally excited pyrazine revealed that vibration−vibration (V−V) energy transfer to the 00^01 level of CO_2 also occurred, mediated mostly through a long-range, attractive force mechanism.[6] Sharma and Brau[18,19] have used such a long-range interaction model to describe near-resonant V−V energy transfer. For example, scattering probabilities for energy transfer between CO_2 (00^01) and N_2 ($v = 1$) are characterized by an inverse temperature dependence in which the excitation probability increases as the temperature decreases, a clear signature of long-range attractive-force energy-transfer processes. This behavior has been observed experimentally for a variety of systems in addition to CO_2/N_2, such as the deactivation of hydrogen halides with different bath molecules.[20−22]

The Sharma−Brau long-range, V−V energy-transfer model has also been applied successfully to the probability of scattering into the low rotational states ($J = 0-40$) of the antisymmetric (00^01) stretch level of CO_2 after collisions with highly vibrationally excited pyrazine.[6] In contrast to this near-resonant energy-transfer process that characterizes the excitation of the low rotational states of CO_2 (00^01) by hot pyrazine, evidence for a slightly more repulsive-force energy-transfer mechanism was also observed for scattering into the higher rotational states ($J > 41$) of the CO_2 00^01 vibrational state. These scattering events exhibit a probability that is essentially flat with temperature.

In the present work, the excitation of the CO ($v = 1, J$) levels due to collisions with highly vibrationally excited pyrazine has been studied for the purpose of determining the importance as well as the mechanism for these collision events. The experiments reveal a detailed picture of the rotational as well as translational excitation of CO molecules scattered into the first vibrational state. A comparison of these findings with results for the collisional excitation of the (00^01) antisymmetric stretch

† Part of the special issue "A. C. Albrecht Memorial Issue".

‡ Present address: New York School of Medicine, New York, NY 10016.

10.1021/jp0225626 CCC: $25.00
Published on Web 06/24/2003

state in CO_2 provides further insight into the mechanism for quenching highly vibrationally excited molecules.

Experimental Section

The diode laser probe technique, used here to study collisional energy transfer, is described in detail in previous work.[5−9,16,23,24] Briefly, a constant amount of a pyrazine/CO gas mixture flows through a 3-m-long jacketed, insulated cell, which is maintained at constant pressure by an MKS flow control system. Total gas pressure is adjusted to obtain a mean gas kinetic collision time of 4 μs. The optimum ratio of pyrazine and CO was found to be approximately 1:2 for maximum signal. Partial pressures of pyrazine and CO are verified by measuring their UV and IR absorption, respectively. Experiments are performed between 247 and 339 K by circulating methanol refrigerant (FTS Kinetics refrigerator) or hot water (Neslab Instruments heater) through a glass-jacketed cell.

A 248 nm KrF excimer laser (Lambda Physik), operating at 0.5 Hz, is used to excite the pyrazine:

$$\text{pyrazine} + h\nu\ (248\ \text{nm}) \rightarrow \text{pyrazine}^* \qquad (1)$$

Pyrazine* then transfers energy to the CO bath molecules through collisions:

$$\text{pyrazine}^* + \text{CO}\ (v = 0) \rightarrow \text{CO}\ (v = 1, J, V) + \text{pyrazine} \qquad (2)$$

where v is a specific vibrational state, J is the final rotational state, and V is the final lab frame recoil velocity. Scattered CO ($v = 1$) is probed with a continuous-wave IR diode laser (Laser Analytics):

$$\text{CO}\ (v = 1, J, V) + h\nu\ (4.8\ \mu\text{m}) \rightarrow \text{CO}\ (v = 2, J \pm 1, V) \qquad (3)$$

The IR diode laser beam is propagated collinearly with the UV light (by use of a dichroic beam splitter) through the collision cell and directed through a monochromator to a liquid N_2-cooled InSb detector (Santa Barbara Research). The IR transient signal is displayed on a digital oscilloscope (LeCroy), which is connected to a PC (Gateway) for subsequent data storage and analysis.

The scattered population of vibrationally excited CO in a specific rotational state is obtained from transient absorption signals, which are measured by locking the diode laser to the center of a CO rotational line of the $v = 1 \rightarrow v = 2$ vibrational transition. For this purpose approximately 10% of the IR light is directed through a gas discharge reference cell containing CO, to an additional InSb detector, which is connected to a lock-in amplifier (Stanford Research Systems). A feedback loop between the diode controller and the lock-in amplifier keeps the diode laser frequency precisely at the center of a specific CO line in the reference cell during data collection. The vibrationally excited CO in the reference cell, which is used for locking the diode frequency, is produced by a high-voltage discharge (~10 kV, 40 mA, DC) through 100 mTorr of N_2 and 60 mTorr of CO.[25] All transients measured for specific rotational states are averaged over 500 excimer laser shots.

For measurements of the CO line width, the diode laser is locked to the fringe of a scanning Fabry−Perot Etalon, which can be placed in the reference cell arm. CO Doppler-broadened line profiles are collected by scanning an Etalon fringe (and, hence, the diode laser) across a CO ($v = 1, J, V$) + $h\nu \rightarrow$ CO ($v = 2, J \pm 1, V$) absorption line near 4.8 μm. Each line shape contains on average 29 data points and each point is averaged over ~100 excimer laser shots.

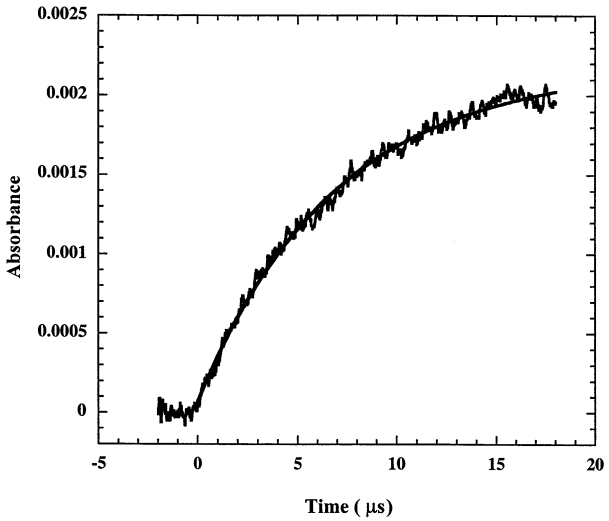

Figure 1. The IR transition CO ($v = 1, J = 6$) → CO ($v = 2, J = 7$) at 2142.47 cm^{-1} is probed after 248 nm excitation of pyrazine at $t = 0$ in a mixture of 6.7 mTorr CO with 13.3 mTorr of Pyrazine. The rise in the transient absorption corresponds directly to an increase in the number density of CO ($v = 1, J = 6$) molecules, due to collisions with highly vibrationally excited pyrazine ($E = 40\,640$ cm^{-1}). The solid line is a smooth fit to the experimental data. The data fit corresponds to a double exponential with the general form $y = -m_5 + m_1 \exp(-m_2 t) + m_3 \exp(-m_4 t)$, where m_1–m_5 are fitting parameters and t is time. The IR transient signal shown here is averaged over 500 excimer laser shots.

In all experiments, the transient absorption by the collisionally excited CO is acquired by a dual-channel detection method. The ratio of the ac- and dc-coupled IR absorption signal is recorded on the digital oscilloscope, which is the equivalent of measuring $\Delta I/I$. This method makes the IR transient absorption independent of small fluctuations in the diode laser intensity.

CO spectral grade gas from Spectra Gases (99.995%) was used in the experiments. Pyrazine (Aldrich, 99+%) was purified via several freeze−pump−thaw cycles.

Results

(1) Rotational Excitation of CO ($v = 1$). After a collision with highly vibrationally excited pyrazine, a small percentage of CO molecules are excited into the first vibrational level. Other CO/pyrazine experiments confirm that the dominant energy-transfer mechanism is the scattering of CO into high rotational states of the ground ($v = 0$) level ($J = 20-36$).[17] The same trend was also observed in collisions of highly vibrationally excited donors with CO_2,[7,8,16,24] and similar results have been obtained for CO/pyrazine collisions from trajectory calculations.[13]

In contrast to the CO($v = 0$) ground vibrational state,[17] the present experiments focus on probing rotational states of CO ($v = 1$) near the center of the room-temperature Boltzmann distribution, which corresponds to a most probable rotational state of $J = 7$ ($T = 300$ K). The small signal-to-noise ratio, arising from the relatively small number of CO molecules scattered into $v = 1$, allowed us to record transient absorption signals only between $J = 4$ and $J = 18$. A typical transient signal for scattering into CO ($v = 1, J = 6$), which was probed through the following transition in the R branch:

$$\text{CO}\ (v = 1, J = 6) + h\nu\ (4.8\ \mu\text{m}) \rightarrow \text{CO}\ (v = 2, J = 7) \qquad (4)$$

is displayed in Figure 1. The excimer laser fires at $t = 0$, and the change in absorption can be directly viewed as an increase in the population of CO ($v = 1$, $J = 6$). In contrast to transients obtained for scattering into high rotational states of the ground ($v = 0$) vibrational level, transients for scattering into $v = 1$ show a slower rise time.

Due to the small signal-to-noise ratio, the absorption at 1 μs after the excimer laser pulse was determined through an exponential fitting method rather than by reading the 1 μs amplitude value directly off the oscilloscope. Figure 1 includes a double-exponential fit to the experimentally measured transient absorption signal. The absorption amplitude at 1 μs is equivalent to the slope of the double-exponential fit at $t = 0$. The following equation is used to fit the experimentally measured transients:

$$y = -m_5 + m_1 \, e^{-m_2 t} + m_3 e^{-m_4 t} \tag{5}$$

where y is the transient absorption amplitude, m_1–m_5 are the parameters of the fit, and t is the time in microseconds. The initial slope of the double exponential corresponds to the derivative of the fitting function at $t = 0$, which is expressed as

$$\left.\frac{dy}{dt}\right|_{t=0} = -m_2 m_1 e^{-m_2 t} - m_4 m_3 e^{-m4t}|_{t=0} = -m_2 m_1 - m_4 m_3 \tag{6}$$

For the small signals in the present experiments, eq 6 is equivalent to $y(t) - y(0)$ evaluated at $t = 1$ μs.

The absorption values determined from these exponential fits generally agree within 30% with the values measured directly off the oscilloscope at 1 μs. These differences are the result of noise fluctuations in the transient absorption signal. For example, inspection of the absorption at $\Delta t = 1$ μs in Figure 1 shows a slight difference between the value for the absorption determined from the fitted exponential compared to the value obtained from the noisy experimental curve.

The IR absorption for each J state measured is used to calculate the rotational population for CO molecules scattered into a specific rotational state in the first vibrational ($v = 1$) level after a collision with highly vibrationally excited pyrazine. A plot of the logarithm of population/($2J + 1$) versus the rotational energy is used to determine the rotational temperature of the CO molecules scattered into the first ($v = 1$) vibrational state. Figure 2 shows these "Boltzmann plots" for three different initial cell temperatures. In each case the rotational temperature is approximately equal to the initial cell temperature, indicating that the transfer of vibrational energy from pyrazine to CO ($v = 1$) is not accompanied by any significant rotational excitation of the CO bath molecules. In addition, within experimental error, we cannot detect a difference in slope for the low J states (4−11) and the high J states (12−18) in the Boltzmann plot. A slight change in the slope of the Boltzmann plot for higher rotational states was observed for CO_2 molecules scattered into the 00^01 state after a collision with highly vibrationally excited pyrazine.[6] Although a similar trend is expected for CO molecules transferred into $v = 1$, this effect cannot be seen clearly in the data, due to the scatter in the experimental points arising from the relatively small signals. The quality of the transient absorption signals deteriorates with increasing J due to the drop in population with J, thereby limiting the experiments to rotational states no higher than $J = 18$. [The absorption cross section for CO ($v = 1 \rightarrow 2$) is approximately a factor of 10 smaller than that for CO_2 ($00^01 \rightarrow 00^02$), which contributes to the relative difficulty of probing high J states of CO compared to CO_2.]

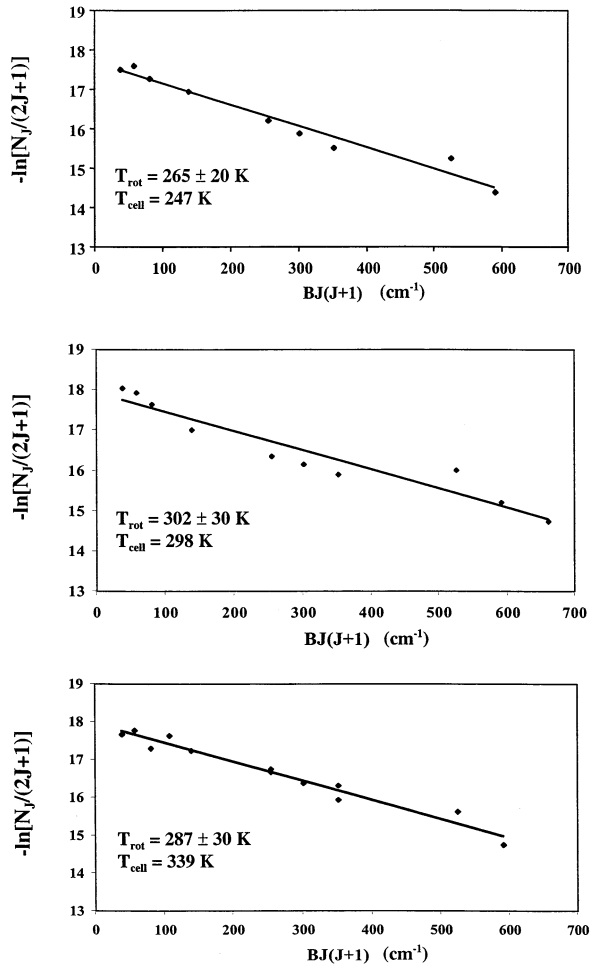

Figure 2. "Boltzmann plots" for CO scattered into $v = 1$ after collision with highly vibrationally excited pyrazine at three different initial cell temperatures. The y axis corresponds to ln [N_J/($2J + 1$)], where N_J is equal to the population of CO ($v = 1$, J), and the x axis is the rotational energy $BJ(J + 1)$. The slope of a linear least-squares fit line corresponds to $-B/kT_{rot}$, where $B = 1.931$ cm^{-1} is the rotational constant for CO, k is the Boltzmann constant, and T_{rot} is the rotational temperature, which was calculated for all three initial cell temperatures. The error limits for all T_{rot} were determined from the standard deviation in the slope of the linear least-squares fit.

(2) Translational Excitation of CO ($v = 1$). Doppler-broadened line profiles were obtained (at $t = 1$ μs after excitation of pyrazine by 248 nm laser light) for the transition CO ($v = 1$, $J = 6$) → CO ($v = 2$, $J = 7$) at cell temperatures of 247, 298, and 339 K. The measured line shapes and their Gaussian fits are displayed in Figure 3. In contrast to the CO ($v = 0$) ground-state transitions CO($v = 0$, J) → CO ($v = 1$, $J \pm 1$), the full width half-maxima (fwhm) of the infrared transition line widths for CO molecules scattered into $v = 1$ show no significant broadening compared to the line shapes calculated from the ambient cell temperatures. The translational temperatures, which can be calculated from eq 7 below, indicate that the translational excitation is small for CO molecules scattered into $v = 1$.

$$T_{trans} = \frac{Mc^2(\Delta\nu_{obs})^2}{8R \ln 2(\nu_0)^2} \tag{7}$$

Here M is the mass of CO, c is the speed of light, $\Delta\nu_{obs}$ is the fwhm of the experimentally measured line, R is the gas constant, and ν_0 is the center frequency of the rotational transition. Although CO molecules scattered into higher J levels of the

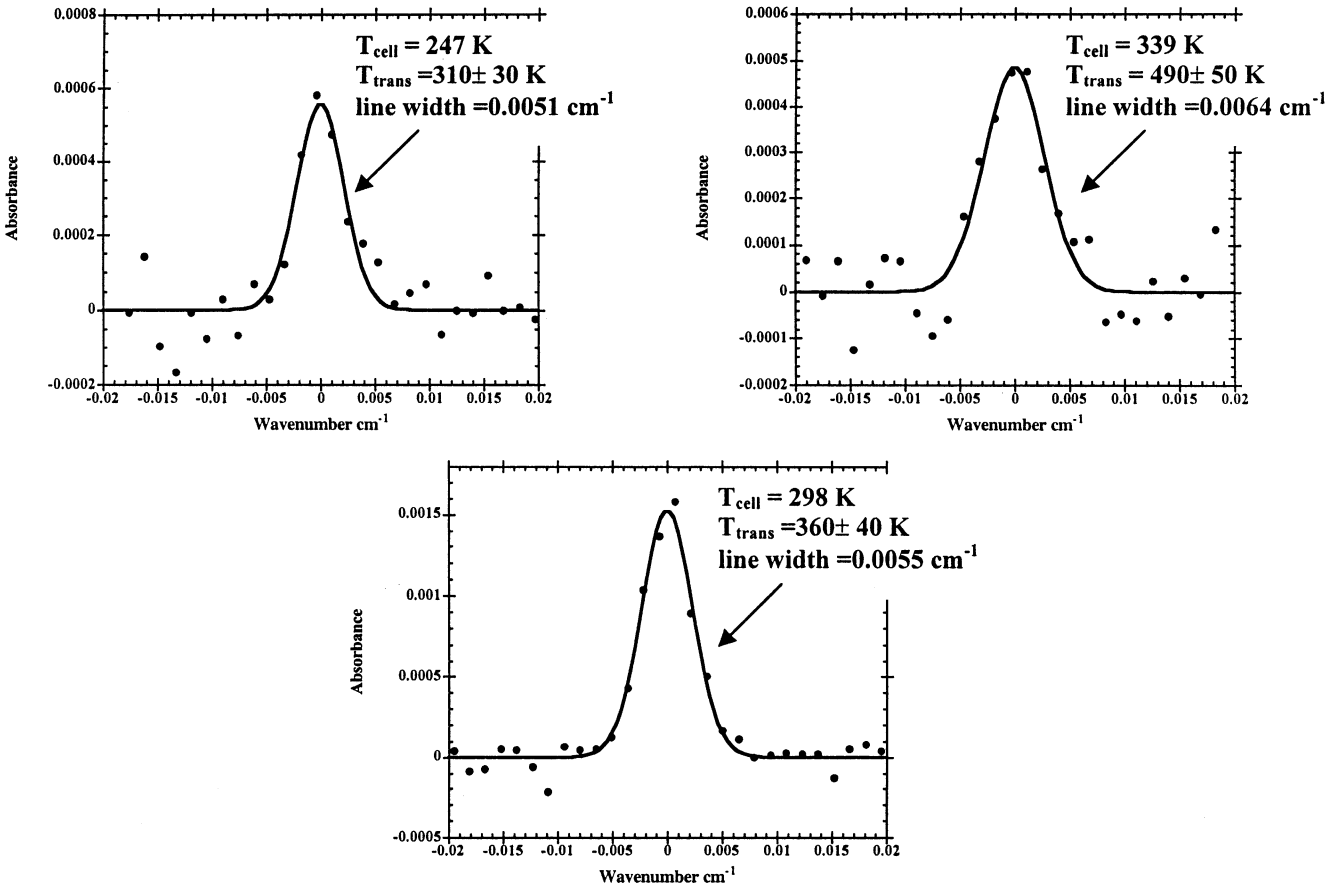

Figure 3. Doppler broadened line profiles for the CO ($v = 1$, $J = 6$) → CO($v = 2$, $J = 7$) transition are shown at three different initial cell temperatures. The experimental data correspond to the solid circles, fitted to a Gaussian line shape represented by the solid line in the plots. The fwhm (full width at half-maximum) was determined from a nonlinear least-squares fit of the data to the Gaussian line profile, and used to calculate T_{Trans} for CO ($v = 1$, $J = 6$) molecules produced by collisions of CO with highly vibrationally excited pyrazine. Each data point corresponds to an average of ~100 excimer laser shots taken at 1 μs after the excimer fires in a gas mixture of total pressure 20 mTorr with a CO:pyrazine ratio of 1:2.

first vibrational state might be expected to exhibit slightly more translational excitation than molecules scattered into the low J states of $v = 1$, the small signals in these high J levels made line width measurements for these states difficult to obtain.

(3) Final Rotationally Resolved Rate Constants. The number densities of the excited- and ground-state species are used to calculate the rate constant for scattering into a specific rotational state of the first vibrationally excited level of CO. The collisional energy transfer is as follows:

$$\text{pyrazine}^* + \text{CO}\ (v = 0) \rightarrow \text{pyrazine} + \text{CO}\ (v = 1, J, V) \tag{8}$$

The rate of excitation of CO into the first vibrational level can then be described by

$$\frac{\mathrm{d}[\text{CO}\ (v = 1, J, V)]}{\mathrm{d}t} = k_2{}^J[\text{CO}\ (v = 0)][\text{pyrazine}^*] \tag{9}$$

where $k_2{}^J$ is the rate constant for scattering into a specific J state. For single-collision conditions (short times), the above equation can be expanded and rearranged to give

$$k_2{}^J = \frac{[\text{CO}\ (v = 1, J, V)]}{[\text{CO}\ (v = 0)]_0[\text{pyrazine}^*]_0 \Delta t} \tag{10}$$

where $[\text{CO}\ (v = 0)]_0$ is the initial bulk density of CO, $[\text{pyrazine}^*]_0$ is the density of pyrazine excited by the excimer pulse at $t = 0$, and Δt is the time interval after $t = 0$ at which the absorption used to calculate the population [CO ($v = 1$, J, V)] is measured. In these experiments $\Delta t = 1$ μs.

TABLE 1: Experimentally Measured Rate Constants ($k_2{}^J$)[a] for Pyrazine* + CO ($v = 0$) → Pyrazine + CO ($v = 1$, J, V) at Three Different Cell Temperatures

final rotational state J	$k_2{}^J$ at 247 K[b]	$k_2{}^J$ at 298 K[b]	$k_2{}^J$ at 339 K[b]
4	3.5×10^{-14}	8.3×10^{-14}	3.1×10^{-14}
5	4.7×10^{-14}	9.2×10^{-14}	4.2×10^{-14}
6	4.0×10^{-14}	9.0×10^{-14}	3.1×10^{-14}
7			4.9×10^{-14}
8	3.8×10^{-14}	6.8×10^{-14}	3.8×10^{-14}
11	2.4×10^{-14}	4.8×10^{-14}	3.1×10^{-14}
12	1.9×10^{-14}	4.3×10^{-14}	2.4×10^{-14}
13	1.4×10^{-14}	3.5×10^{-14}	2.0×10^{-14}
16	1.4×10^{-14}	4.0×10^{-14}	1.5×10^{-14}
17	6.1×10^{-15}	1.9×10^{-14}	6.5×10^{-15}
18	1.5×10^{-15}	1.3×10^{-14}	

[a] The units for $k_2{}^J$ are cubic centimeters per molecule per second; rate constants are calculated from eq 10 in the text. The error in the rate constants is approximately ±35%. [b] Temperature of the CO/pyrazine gas mixture before energy transfer collisions take place.

The rotationally resolved rate constants calculated in this way can be found in Table 1 for the three different initial cell temperatures studied. The total rate constants for scattering into CO ($v = 1$), which are integrated over the final rotational states, can be found in Table 2. This table also contains the hard-sphere and Lennard-Jones collision numbers and the average amount

TABLE 2: Integrated Rate Constants and Collision Numbers for the Process Pyrazine* + CO ($v = 0$) → Pyrazine + CO ($v = 1$) at Three Different Initial Cell Temperatures

T_{cell} (K)	k_2' [a] (cm^3 molecule^{-1} s^{-1})	k_{HS}/k_2' [b]	k_{LJ}/k_2' [c]	$\langle\Delta E_{vib}\rangle$ [d] (cm^{-1})
247	4.5×10^{-13}	721	1074	2.0
298	9.5×10^{-13}	373	519	4.2
339	4.7×10^{-13}	806	1075	2.0

[a] k_2' is the rotationally integrated rate constant for scattering into CO ($v = 1$) after a collision with highly vibrationally excited pyrazine. The integrated rate constant can be calculated from $k_2^J = k_2'(2J + 1)e^{[-BJ(J+1)/kT_{rot}]}/Q$, where k_2^J is the rotationally state-specific rate constant tabulated in Table 1. Any state-specific rate constant can be used to compute k_2' as long as the CO population scattered into CO ($v = 1$, J) follows the same rotational temperature T_{rot}. The values in the table for each temperature are obtained by averaging the k_2' calculated from k_2^J in Table 1 for all final rotational states. Rotational temperatures (T_{rot}) are obtained from the plots shown in Figure 2. [b] This ratio gives the mean number of hard-sphere collisions required to excite CO ($v = 1$). The hard-sphere collision rate constant is calculated from $k_{HS} = \pi(d_{CO} + d_{pyr}/2)\sqrt{8k_BT/\pi\mu}$, where $d_{CO} = 3.75$ Å, $d_{pyr} = 5.35$ Å, k_B is the Boltzmann constant, and μ is the reduced mass for the CO/pyrazine pair. [c] This ratio gives the mean number of Lennard-Jones collisions required to excite CO ($v = 1$). k_{LJ} is the Lennard-Jones collision rate constant, $k_{LJ} = \pi(d_{CO} + d_{pyr}/2)\sqrt{8k_BT/\pi\mu}(2\epsilon/kT)^{1/3}\Gamma(2/3)$, where $d_{CO} = 3.75$ Å, $d_{pyr} = 5.35$ Å, k_B is the Boltzmann constant, μ is the reduced mass for the CO/pyrazine pair, ϵ is the Lennard-Jones well depth, and Γ is the gamma function. ϵ was obtained from $\epsilon = (\epsilon_{CO}\epsilon_{pyr})^{1/2}$, where $\epsilon_{CO} = 73$ cm^{-1} and $\epsilon_{pyr} = 303$ cm^{-1} were taken from ref 27. [d] $\langle\Delta E_{vib}\rangle$ is the mean energy transferred per Lennard-Jones collision resulting in the excitation of CO ($v = 1$), $\langle\Delta E_{vib}\rangle = (k_2'/k_{LJ})(2170.20$ cm$^{-1})$, where 2170.20 cm^{-1} is the energy of the CO ($v = 1$) vibrational state.

of vibrational energy transferred to CO ($v = 1$) after a collision with highly vibrationally excited pyrazine.

Discussion

(1) Identification of the Energy Transfer Mechanism. One of the main purposes of these experiments was to determine the importance of vibrational excitation of the CO bath molecules arising from collisions with highly vibrationally excited pyrazine and to identify the mechanism of this collisional energy transfer. Previous studies of the deactivation of pyrazine following collisions with CO_2, which produce vibrational excitation in the bath gas, suggest that "soft" encounters (where energy transfer takes place at a distance large compared to the Lennard−Jones characteristic length sigma) are likely to be important for this process.[6,9] In the case of energy transfer to CO_2, most of the CO_2 molecules are scattered into the low ($J = 3-39$) rotational states of the 00^01 level through a long-range attractive force mechanism in which the change in angular momentum for CO_2 going from the (00^00, J) levels to the (00^01, J') levels follows "dipole selection rules" ($\Delta J = J' - J = \pm 1$). The translational recoil of the CO_2 molecules [measured through the Doppler profiles of the CO_2 (00^01, J) → CO_2 (00^02, $J \pm 1$) infrared transitions] was also found to be small, consistent with a soft-collision energy-transfer picture. The small change in angular momentum and the small recoil velocity are the signature of resonant vibrational energy transfer in which vibrational energy initially contained in the pyrazine molecule is exchanged for vibrational energy in the CO_2 molecule with little or no energy going into the translational or rotational degrees of freedom.

In the present study, the rotational and translational excitation of CO ($v = 1$) due to collisions with hot pyrazine was analyzed (see Figures 2 and 3), and the measured rotational and translational temperatures for the CO($v = 1$, $J = 4-18$) states were found to be only slightly above their ambient values. As in the case of CO_2, these data provide clear evidence for a dominant long-range energy-transfer mechanism in which vibrational excitation in hot pyrazine is exchanged for vibrational energy in the cold CO bath molecules via "soft" collisions.

In the case of collisional excitation of carbon dioxide by hot pyrazine, evidence was also found for a less important energy-transfer mechanism that led to production of high J states in (00^01). The levels (00^01, J) with $J = 41-55$ were found to be characterized by a rotational temperature slightly above that for the levels from $J = 3-39$, indicating excitation via slightly harder, more rotationally inelastic collisions.[6] Given a most probable J of 16 for the CO_2(00^00) level at room temperature, the decreasing importance of producing (00^01, $J > 41$) from (00^00, J) via a mechanism with $\Delta J = \pm 1$ is not surprising. The population in the initial feeder states for such a mechanism (00^00, $J > 40$) decreases rapidly with J, which in turn decreases the importance of any mechanism originating from these states. In contrast rotationally inelastic (harder collision) events that produce (00^01, $J > 41$) from feeder levels such as (00^00, $J \sim 16-30$) would be favored for these high J levels.

In the present study, the rotational temperature plots for CO ($v = 1$) showed no evidence of different slopes for the lower ($J = 4-11$) and higher ($J = 13-18$) rotational states probed in the experiment. This is probably not surprising as CO ($v = 1$) states with $J = 13-18$ can still be fed via a $\Delta J = \pm 1$ mechanism from CO ($v = 0$) states that have significant population, since the most probable and the average rotational states (J) for CO near room temperature are 7 and 10, respectively. Due to the small signals in the present experiments, states above CO ($v = 1$, $J = 18$), where rotationally inelastic events might be expected to be more important, could not be probed. [A comparison of the population ratios CO ($v = 0$, $J = 13$)/CO ($v = 0$, $J = 7$) to CO_2 (00^00, $J = 42$)/CO_2 (00^00, $J = 16$) and CO ($v = 0$, $J = 18$)/CO ($v = 0$, $J = 7$) to CO_2 (00^00, $J = 56$)/CO_2 (00^00, $J = 16$) indicates roughly that the onset of the more inelastic mechanism ought to take place beginning at CO ($v = 1$, $J = 18$), assuming only population factors are important in determining the relative importance of this mechanism compared to the long-range process.)

The rate constants defined by eqs 9 and 10 and presented in Table 1 show considerable variation with J state. However, because the transition moment for the CO ($v = 0 \rightarrow 1$) transition is essentially independent of J for $J \geq 5$, the rate constants for a soft-collision energy-transfer mechanism, mediated by this infrared transition moment, would also be expected to be almost J-independent. The apparent variation of the energy transfer rate constant in Table 1 arises from the use in eq 10 of the *total* ground-state population, $[CO\ (v = 0)]_0$, in the expression for k_2^J. This definition is consistent with the normal assumption in kinetic rate equations that the *total* initial population is available for a given scattering event. For a soft-collision-mediated process, on the other hand, the state CO ($v = 1$, J) can only be reached from the two states CO ($v = 0$, $J + 1$) and CO ($v = 0$, $J - 1$) due to the restrictions imposed by the dipole selection rules. Thus, in eq 10 if we replace $[CO\ (v = 0)]_0$ by the more restricted initial feeder state populations $[CO\ (v = 0, J + 1)]_0 + [CO\ (v = 0, J - 1)]_0$, the apparent variation in k_2^J would all but disappear. In fact the Boltzmann temperature plots in Figure 2 are a signature of the variation in the $[CO\ (v = 0, J + 1)]_0 + [CO\ (v = 0, J - 1)]_0$ populations, which are the feeder states for scattering into CO ($v = 1$, J). Thus, the apparent variation

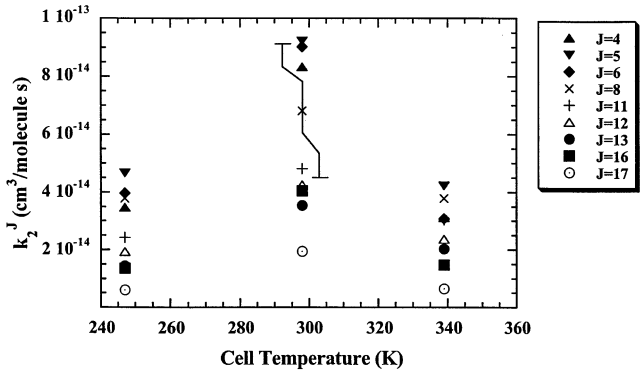

Figure 4. Shown is the temperature dependence of the rate constant, k_2^J, for scattering of CO ($v = 0$) → CO ($v = 1$, J) at three cell temperatures for eight different final rotational states. k_2^J is defined in eq 9 in the text. The error bar shown represents typical fluctuations found for a single J state at different cell temperatures.

in the individual k_2^J rate constants really reflects the variation in the population of ground-state molecules, CO ($v = 0$, J), since the probability for a CO ($v = 0 \rightarrow 1$) scattering transition is essentially independent of J for a dipole transition-moment-mediated process.

The cell temperature dependence of the rotationally resolved rate constants, k_2^J, provides a less clear picture of the mechanism than in the case of CO_2.[6] Figure 4 shows a plot of the experimentally measured rate constants, k_2^J, for CO at three different cell temperatures. The rate constants for all final J states exhibit the same type of fluctuation as a function of cell temperature, with the room-temperature rate constant for all measured final rotational states being slightly larger than the values at 247 and 339 K. Nevertheless, the error limits for the measurements at different temperatures are significant (±35%), and the changes in probabilities with temperature must be considered essentially flat.[26] Previous pyrazine collisional cooling experiments with CO_2 as the bath clearly showed an inverse temperature dependence (probability increasing as temperature decreases) for scattering into the lowest J states (e.g., $J = 15$ and 17) in the 00^01 level.[6] In contrast scattering into higher J states ($J = 35-50$) exhibited an essentially flat temperature dependence, similar to that observed here for the CO ($v = 1$, J) levels with J running from 4 to 17.

A decrease of the J-dependent rate constants with increasing temperature is usually linked to a long-range attractive-force energy-transfer mechanism.[6,18,19,22] The behavior of all rate constants for CO molecules scattered into $v = 1$ show temperature fluctuations that appear to be relatively flat, a dependence that might be expected for a mixed repulsive/attractive-force mechanism, since the repulsive force mechanism has a probability that increases with temperature in contrast to the behavior for the attractive force process. The difference in temperature behavior between CO and CO_2 may be related to the differences in their infrared transition moment squared, which is smaller by a factor of 10 for CO($v = 0 \rightarrow v = 1$) than for CO_2 ($00^00 \rightarrow 00^01$). On average, this must necessarily lead to CO($v = 0$, $J \rightarrow v = 1$, $J \pm 1$) collisional excitations that take place at shorter range for CO than the analogous CO_2 (00^00, $J \rightarrow 00^01$, $J \pm 1$) collisional scattering. It is interesting to note that in both the CO and CO_2 cases, final J states that exhibit a flat temperature dependence for the excitation probabilities ($J = 4-17$ for CO and $J = 35-50$ for CO_2) are characterized by cool rotations and translations, a very clear sign of "soft" collision energy transfer.

(2) Comparison of the Energy Transfer Probabilities for Scattering into CO ($v = 1$) and CO_2 (00^01) Due to Collisions with Highly Vibrationally Excited Molecules. Table 3 shows the Lennard-Jones probabilities for scattering into specific rotational states of the first excited level of CO. On average all P_{LJ} for CO are almost an order of magnitude lower than the probabilities determined for CO_2 scattered into the 00^01 level.[6] In fact, the Lennard-Jones probabilities integrated over all final rotational states, which can also be found in Table 3, show that only 0.1% of the CO molecules are excited into the first vibrational state in the deactivation of highly vibrationally excited pyrazine. A comparison of the integrated P_{LJ}'s for CO and CO_2 in Table 3 shows that the excitation of the 00^01 level of CO_2 is approximately 5−10 times more efficient compared to the excitation of $v = 1$ of CO. A resonant vibrational energy exchange between pyrazine and CO_2 or CO would be expected to have a probability that scales like the infrared band strengths (squares of the infrared transition moments) for the CO_2 ($00^00 \rightarrow 00^01$) and CO ($v = 0 \rightarrow 1$) infrared transitions. As noted above, the band strength for CO is approximately 10 times smaller than that for CO_2, in excellent qualitative agreement with this picture. Resonant energy transfer processes such as this are also known to be sensitive to the energy mismatch between the vibrational levels of the donor and the acceptor. In comparing energy transfer from hot pyrazine to CO ($v = 1$) with transfer from hot pyrazine to CO_2 (00^01), such factors are not likely to play an important role. First, the energy gaps for the acceptor molecules are rather similar (2170 cm^{-1} for CO and 2349 cm^{-1} for CO_2). Even this relatively small difference might be significant except for the second factor, which is the high density of vibrational states for hot pyrazine in the experiments (in excess of 10^{14} states/cm^{-1} at the donor energy of 40 640 cm^{-1}). This virtually guarantees that the pyrazine vibrational energy loss will match exactly the energy gain in the acceptor for any transfer in the range 0−3000 cm^{-1}. The relevant matrix elements for donor pyrazine in the two experiments may differ, of course, but there is little information available to assess the importance of such changes at the present time. Such effects are likely to be small for gaps that differ by only 2349 − 2170 = 179 cm^{-1}.

TABLE 3: Final Rotational State Specific and Rotationally Integrated Lennard-Jones Probabilities for Excitation of CO ($v = 1$, J) Due to Collisions with Pyrazine*

final rotational state J	$prob_{LJ}$[a] at 247 K[b]	$prob_{LJ}$[a] at 298 K[b]	$prob_{LJ}$[a] at 339 K[b]
4	7.2×10^{-5}	1.7×10^{-4}	6.2×10^{-5}
5	9.7×10^{-5}	1.9×10^{-4}	8.4×10^{-5}
6	8.2×10^{-5}	1.8×10^{-4}	6.1×10^{-5}
7			9.8×10^{-5}
8	7.9×10^{-5}	1.4×10^{-4}	7.5×10^{-5}
11	5.0×10^{-5}	9.7×10^{-5}	6.0×10^{-5}
12	4.0×10^{-5}	8.6×10^{-5}	4.7×10^{-5}
13	3.0×10^{-5}	7.2×10^{-5}	4.0×10^{-5}
16	2.8×10^{-5}	8.2×10^{-5}	2.9×10^{-5}
17	1.3×10^{-5}	3.9×10^{-5}	1.3×10^{-5}
18	3.2×10^{-6}	2.6×10^{-5}	
Rotationally Integrated P_{LJ} for CO			
	9.3×10^{-4}	1.93×10^{-3}	9.3×10^{-4}
Rotationally Integrated P_{LJ} for CO_2			
	9.5×10^{-3}	7.2×10^{-3}	5.1×10^{-3}
Ratio CO_2/CO			
	10	4	5

[a] $Prob_{LJ} = k_2^J/k_{LJ}$, where k_2^J is the measured state-specific rate constant given in Table 1, and k_{LJ} is the Lennard-Jones gas kinetic collision rate constant calculated as described in footnote *c* of Table 2. [b] Initial temperature of the CO/pyrazine gas mixture before energy transfer collisions take place.

Conclusion

The excitation of CO ($v = 1$) after a collision with highly vibrationally excited pyrazine has been investigated. Both the rotational and the translational excitation of the CO bath molecules were very small, with rotational and translational temperatures for the CO($v = 1$) level only slightly above ambient temperature. In addition, the rotationally resolved rate constants for excitation of CO ($v = 1$, J) were obtained at three different cell temperatures. The rate constants, k_2^J, and Lennard-Jones probabilities, P_{LJ}, for excitation of all final rotational states showed similar weak fluctuations with increasing cell temperature. Similar to results found for CO_2/pyrazine collisions, the energy-transfer mechanism for scattering into all final J states of CO ($v = 1$) appears to occur through a long-range force (soft collision) mechanism. The rotationally integrated rate constants for excitation of CO by collisions with highly vibrationally excited pyrazine were roughly 10 times smaller for CO compared to CO_2. This scaling is close to that predicted for a process mediated by the infrared transition moment (squared) for CO ($v = 0 \rightarrow 1$) and CO_2 ($00^00 \rightarrow 00^01$) vibrational excitation. Only 0.1% of the CO molecules are scattered into the first vibrational level after a collision with highly vibrationally excited pyrazine, making this a minor channel for loss of energy from pyrazine in collisions with CO.

Acknowledgment. The scientific work and the personal characteristics of Andy Albrecht have been an inspiration to the spectroscopic and dynamics communities. We celebrate his memory and mourn his loss. We thank Professor Sally Chapman and Dr. Quan Ju for a number of informative and stimulating discussions. This work was supported by the Department of Energy under Grant DE FGO2 88 ER 13937.

References and Notes

(1) Luther, K.; Reihs, K. *Ber. Bunsen-Ges. Phys. Chem.* **1988**, *92*, 442−445.

(2) Hold, U.; Lenzer, T.; Luther, K.; Reihs, K.; Symonds, A. C. *J. Chem. Phys.* **2000**, *112*, 4076−4089.

(3) Lenzer, T.; Luther, K.; Reihs, K.; Symonds, A. C. *J. Chem. Phys.* **2000**, *112*, 4090−4110.

(4) Miller, L. A.; Cook, C. D.; Barker, J. R. *J. Chem. Phys.* **1996**, *105*, 3012−3018.

(5) Khan, F. A.; Kreutz, T. G.; Flynn, G. W.; Weston, R. E., Jr. *J. Chem. Phys.* **1990**, *92*, 4876−4886.

(6) Michaels, C. A.; Mullin, A. S.; Flynn, G. W. *J. Chem. Phys.* **1995**, *102*, 6682−6695.

(7) Mullin, A. S.; Michaels, C. A.; Flynn, G. W. *J. Chem. Phys.* **1995**, *102*, 6032−6045.

(8) Michaels, C. A.; Lin, Z.; Mullin, A. S.; Tapalian, C. H.; Flynn, G. W. *J. Chem. Phys.* **1997**, *106*, 7055−7071.

(9) Michaels, C. A.; Mullin, A. S.; Park, J.; Chou, J. Z.; Flynn, G. W. *J. Chem. Phys.* **1998**, *108*, 2744−2755.

(10) Lenzer, T.; Luther, K.; Troe, J.; Gilbert, R. G.; Lim, R. G. *J. Chem. Phys.* **1995**, *103*, 626−641.

(11) Bernshtein, V.; Oref, V. *J. Chem. Phys.* **1996**, *104*, 1958−1965.

(12) Bernshtein, V.; Oref, I.; Lendvay, G. *J. Phys. Chem. A* **1997**, *101*, 2445−2450.

(13) Higgins, C.; Ju, Q.; Seiser, N.; Flynn, G. W.; Chapman, S. *J. Phys. Chem. A* **2001**, *105*, 2858−2866.

(14) Clary, D. C.; Gilbert, R. G.; Bernshtein, V.; Oref, I. *Faraday Discuss.* **1995**, *102*, 423−433.

(15) Drabbels, M.; Wodtke, A. M. *J. Phys. Chem. A* **1999**, *103*, 7142−7154.

(16) Sevy, E. T.; Rubin, S. M.; Lin, Z.; Flynn, G. W. *J. Chem. Phys.* **2000**, *113*, 4912−4932.

(17) Seiser, N.; Ju, Q.; Kavita, K.; Flynn, G. W. Manuscript in preparation.

(18) Sharma, R. D.; Brau, C. A. *Phys. Rev. Lett.* **1967**, *19*, 1273−1275.

(19) Sharma, R. D.; Brau, C. A. *J. Chem. Phys.* **1969**, *50*, 924−930.

(20) Lucht, R. A.; Cool, T. A. *J. Chem. Phys.* **1974**, *60*, 1026−1035.

(21) Bott, J. F. *J. Chem. Phys.* **1974**, *60*, 427−434.

(22) Zittel, P. F.; Moore, C. B. *J. Chem. Phys.* **1973**, *59*, 6636−6640.

(23) Flynn, G. W.; Weston, R. E., Jr. *J. Phys. Chem.* **1993**, *97*, 8116−8127.

(24) Mullin, A. S.; Park, J.; Chou, J. Z.; Flynn, G. W.; Weston, R. E., Jr. *Chem. Phys.* **1993**, *175*, 53−70.

(25) Dang, C.; Reid, C.; Garside, B. K. *Appl. Phys. B.* **1982**, 145−151.

(26) At a given temperature, the error in measuring the relative populations of individual J states is reduced by measuring the absorption on a particular CO ($v = 1$, J) → CO ($v = 2$, $J \pm 1$) transition interleaved about every 10 min with a measurement of the CO ($v = 1$, $J = 6$) → CO ($v = 2$, $J = 7$) "indicator line" transition. This produces data pairs giving the ratio of measured populations [CO ($v = 1$, J)/CO ($v = 1$, $J = 6$)]. Given the close proximity in time of the measurements, this approach reduces errors due to excimer laser intensity fluctuations and window fogging arising from buildup of photoproducts in the cell. Unfortunately, a similar approach cannot be used in comparing population ratios (essentially values of k_2^J) at different temperatures.

(27) Miller, L. A.; Barker, J. R. *J. Chem. Phys.* **1996**, *105*, 1383−1391.